Lattice Gas Methods for Partial Differential Equations

A Volume of Lattice Gas Reprints and Articles, Including Selected Papers from the Workshop on Large Nonlinear Systems, Held August, 1987 in Los Alamos, New Mexico

Edited by
Gary D. Doolen, Uriel Frisch, Brosl Hasslacher, Steven Orszag and Stephen Wolfram

Proceedings Volume IV

ROUTLEDGE

LATTICE GAS METHODS FOR PARTIAL DIFFERENTIAL EQUATIONS

LATTICE GAS METHODS FOR PARTIAL DIFFERENTIAL EQUATIONS

A VOLUME OF LATTICE GAS REPRINTS AND ARTICLES, INCLUDING SELECTED PAPERS FROM THE WORKSHOP ON LARGE NONLINEAR SYSTEMS, HELD AUGUST, 1987 IN LOS ALAMOS, NEW MEXICO

Edited by

Gary D. Doolen
Los Alamos National Laboratory

Uriel Frisch
Observatoire de Nice, France

Brosl Hasslacher
Los Alamos National Laboratory

Steven Orszag
Princeton University

Stephen Wolfram
University of Illinois

Proceedings Volume IV

SANTA FE INSTITUTE
STUDIES IN THE SCIENCES OF COMPLEXITY

Routledge
Taylor & Francis Group
LONDON AND NEW YORK

First published 1990 by Westview Press

Published 2018 by Routledge
52 Vanderbilt Avenue, New York, NY 10017
2 Park Square, Milton Park, Abingdon, Oxon OX14 4RN

Routledge is an imprint of the Taylor & Francis Group, an informa business

Library of Congress Cataloging-in-Publication Data

Lattice Gas Methods for Partial Differential Equations
edited by Gary D. Doolen ... [et al.]
p. cm.—(Santa Fe Institute studies in the sciences of complexity; v. 4)
Proceedings of the Workshop on Large Nonlinear Systems, Los Alamos, New Mexico
Includes index.
ISBM 0-201-15679-2.—IBSN 0-201-13232-X (pbk.)
1. Differential equations, Partial. 2. Lattice gas. I. Doolen, Gary D. II. Series.
QA374.L34 1989 515.3'53–dc19 89-30691

ISBN 13: 978-0-367-00287-9 (hbk)

About the Santa Fe Institute

The *Santa Fe Institute* (SFI) is a multidisciplinary graduate research and teaching institution formed to nurture research on complex systems and their simpler elements. A private, independent institution, SFI was founded in 1984. Its primary concern is to focus the tools of traditional scientific disciplines and emerging new computer resources on the problems and opportunities that are involved in the multidisciplinary study of complex systems—those fundamental processes that shape almost every aspect of human life. Understanding complex systems is critical to realizing the full potential of science, and may be expected to yield enormous intellectual and practical benefits.

All titles from the *Santa Fe Institute Studies in the Sciences of Complexity* series will carry this imprint which is based on a Mimbres pottery design (circa A.D. 950–1150), drawn by Betsy Jones.

Santa Fe Institute Studies in the Sciences of Complexity

PROCEEDINGS VOLUMES

Volume	Editor	Title
I	David Pines	Emerging Syntheses in Science, 1987
II	Alan S. Perelson	Theoretical Immunology, Part One, 1988
III	Alan S. Perelson	Theoretical Immunology, Part Two, 1988
IV	Gary D. Doolen et al.	Lattice Gas Methods of Partial Differential Equations
V	Philip W. Anderson et al.	The Economy as an Evolving Complex System
VI	Christopher G. Langton	Artificial Life: Proceedings of an Interdisciplinary Workshop on the Synthesis and Simulation of Living Systems
VII	George I. Bell & Tom Marr	Computers and DNA

LECTURES VOLUMES

Volume	Editor	Title
I	Daniel L. Stein	Lectures in the Sciences of Complexity

Contributors to This Volume

Bruce J. Bayly
Applied and Computational Mathematics, Princeton University

P.-M. Binder
Center for Nonlinear Studies, Los Alamos National Laboratory

B. M. Boghosian
Thinking Machines Corporation

Hudong Chen
Center for Nonlinear Studies, Los Alamos National Laboratory

Shiyi Chen
Center for Nonlinear Studies, Los Alamos National Laboratory

P. Clavin
Combustion Research Laboratory, University of Provence

Andre Clouqueur
Laboratoire de Physique, École Normale Supérieure

A. Despain
JASON, Mitre Corporation

Dominique d'Humières
Physics Laboratory, École Normale Supérieure

K. Diemer
Center for Nonlinear Studies, Los Alamos National Laboratory

Gary D. Doolen
Center for Nonlinear Studies, Los Alamos National Laboratory

Uriel Frisch
Centre National de la Recherche Scientifique, Observatoire de Nice

Castor Fu
Center for Nonlinear Studies, Los Alamos National Laboratory

Brosl Hasslacher
Los Alamos National Laboratory

Tudatsugu Hatori
Department of Physics and Astronomy, Dartmouth College

Victor Hayot
Ohio State University

Michel Hénon
Centre National de la Recherche Scientifique, Observatoire de Nice

K. Hunt
Center for Nonlinear Studies, Los Alamos National Laboratory

Leo P. Kadanoff
The Research Institutes, The University of Chicago

Jeffrey M. Keller
Massachusetts Institute of Technology

Pierre Lallemand
Physics Laboratory, École Normale Supérieure

Y. C. Lee
Center for Nonlinear Studies, Los Alamos National Laboratory

C. D. Levermore
Lawrence Livermore Laboratory

Norman Margolus
MIT Laboratory for Computer Science

William H. Matthaeus
Bartol Research Institute, University of Delaware

C. E. Max
JASON, Mitre Corporation

Guy R. McNamara
The Research Institutes, The University of Chicago

David Montgomery
Dartmouth College

Steven A. Orszag
Princeton University

Yves Pomeau
Physics Laboratory, École Normale Supérieure

Jean-Pierre Rivet
École Normale Supérieure

Daniel H. Rothman
Massachusetts Institute of Technology

Geoffrey Searby
Laboratoire de recherche sur la combustion

Tsutomu Shimomura
Los Alamos National Laboratory

Tommaso Toffoli
MIT Laboratory for Computer Science

Stephen Wolfram
Center for Complex Systems Research and
University of Illinois

Victor Yakhot
Princeton University

Gianluigi Zanetti
The Research Institutes, The University of Chicago

Gary Doolen
Los Alamos National Laboratory, Los Alamos, NM 87545

Preface

MOTIVATION

Although the idea of using discrete methods for modeling partial differential equations occurred very early, the actual statement that cellular automata techniques can approximate the solutions of hydrodynamic partial differential equations was first discovered by Frisch, Hasslacher, and Pomeau. Their description of the derivation, which assumes the validity of the Boltzmann equation, appeared in the *Physical Review Letters* in April 1986. It is the intent of this book to provide some overview of the directions that lattice gas research has taken from 1986 to early 1989.

There are several reasons for the recent rapid growth in lattice gas research. The method provides very high resolution. Problems with 5,000,000,000 cells can now be run on a CRAY Y/MP. Also, the algorithm is totally parallel. This parallel feature is easily exploited on existing computers. In addition, an enormous gain can be made by constructing dedicated hardware. Already, inexpensive dedicated boards are available which allow small PCs to run lattice gas problems near CRAY speeds. Dedicated boards are now planned for delivery in 1990 which are expected to be a thousand times more powerful. It is possible to build with existing technology a dedicated machine which has the complexity of existing CRAYs but which would execute lattice gas algorithms many millions of times faster. One should interpret

Lattice Gas Methods for Partial Differential Equations, SFI SISOC,
Eds. Doolen et al., Addison-Wesley Publishing Co., 1990

this impressive gain in computer speed cautiously. For periodic problems on existing machines, lattice gas methods are slower than spectral methods at least by an order of magnitude. But for complicated boundary conditions, lattice gas methods can solve problems which are not solvable by other methods. An example is flow through porous media.

At least four separate communities are closely following lattice gas developments with quite different expectations. The molecular dynamics community considers the lattice gas method to be a minimal-bit strategy for solving Newton's equations of motion using orders of magnitude more particles than are usually simulated. Finite difference theorists consider the method to be an over-restricted set of finite difference equations, rightly expecting many finite difference diseases to be amplified. Statistical mechanicians hope to use the method to gain new insight into the relation between microdynamics and macrodynamics. Parallel computer hardware scientists see the method as the simplest and fastest totally parallel algorithm with broad applications.

BOOK OVERVIEW

In the section labeled "Basic Papers," a *Scientific-American*-level reprint of an article by Shimomura, Doolen, Hasslacher, and Fu highlights the principal advantages and some of the limitations of lattice gas methods. Derivations of the hydrodynamic equations are outlined in articles by Wolfram and by Frisch, d'Humieres, Hasslacher, Lallemand, Pomeau, and Rivet. The article by Diemer et al. gives some details of the viscosity and mean free path for several two-dimensional and three-dimensional models. The article by Hénon derives the analytic formula for viscosity from the definition of viscosity. The section on computer hardware begins with a paper which outlines the impressive speed which could be obtained by building a dedicated lattice gas computer with existing hardware. The following article by Margolus and Toffoli describes the CAM-6, an existing computer board which enables a personal computer to achieve supercomputer speeds for small lattice gas systems. This article also describes the CAM-8, a dedicated board now in the design phase. The article by Clouqueur and d'Humières describes the capabilities of the RAP-1, a board with capabilities similar to those of the CAM-6.

The section on hydrodynamic studies and application papers contains a selection of some of the many papers on hydrodynamic applications of the lattice gas method. The power of the method to use minimal computer memory and to conserve exactly the required constants of the motion have been studied in several of these reprints. Many of the articles describe detailed computer simulations, but to date there have not been any articles which describe the codes themselves. A few translations of original French articles are included in this section.

The section on more partial differential equations gives a small sampling of a few of the lattice gas algorithms developed to solve partial differential equations which differ considerably from the Navier-Stokes equations.

Finally, a bibliography including most of the papers which reference the original Frisch, Hasslacher and Pomeau article is provided which includes some abstracts. An attempt was made to include articles through April 1989.

FUTURE CHALLENGES

One can think of the lattice gas method as filling a niche between molecular dynamic methods and continuum methods. A present challenge is to determine the boundaries of parameter space where lattice gas methods are most appropriate. It is possible to add complexity to these methods until the results become indistinguishable from both molecular dynamics and continuum methods. However, the method becomes slower as the complexity increases. At the present time, the lattice gas method appears to be ideal for describing flow through porous media.

The lattice gas algorithm can be shown to approximately solve the Navier-Stokes equations in the long wavelength limit. But the algorithm can go far below this limit and possibly give considerable insight into the correct macroscopic treatment in situations where gradients are important and also in situations where the mean-free path is not negligible. The understanding of how to go from the microscopic rules to the correct macroscopic equations remains a challenge, and the lattice gas has much to contribute here.

Another challenge is to determine the fastest lattice algorithm. At present, table look-up methods are very fast. For example, 300,000,000 sites can now be updated each second on a CRAY X/MP 416. The table size grows, however, as 2 to the Nth power, where N is the number of bits required at each site. For 24-bit models, 16-million-word tables are required. It appears that reduced-size tables are possible, but the restrictions which they place on the collision rules may significantly limit the range of allowed viscosities. Several studies are in progress to determine the class of algorithms which ought to be implemented in the type of dedicated lattice-gas computer described in the first article in this book in the section on computer hardware.

The most significant challenge is the implementation of the lattice gas algorithm on large-scale dedicated hardware. The gain in speed over existing computers is a factor of the order of many millions. This opportunity does not belong exclusively to lattice gas techniques but applies to all algorithms which have a parallel implementation.

INTENDED READERSHIP

The book is assembled to show potential users and lattice gas scientists what research has been completed and to give some indication of the utility and limitations of lattice gas models. Most articles should be readable by students who are considering entering the field or who are contemplating the application or extension of these methods to their favorite problems.

ACKNOWLEDGMENTS

Many people have contributed to the creation of this volume. Any attempt to list them all would necessarily fall short. At various stages, advice and guidance were received gratefully from Uriel Frisch, Brosl Hasslacher, Stephen Orszag, and Stephen Wolfram. Much of the bibliographical work was provided by Dominique d'Humieres and Tsutomu Shimomura. Finally, the essential coordination and typesetting by Ronda Butler-Villa of the Santa Fe Institute is very much appreciated.

Gary Doolen
Center for Nonlinear Studies
Los Alamos National Laboratory
May 1989

Contents

Basic Papers

Tsutomu Shimomura, Gary D. Doolen, Brosl Hasslacher, and Castor Fu
Los Alamos National Laboratory, Los Alamos, NM 87545

Calculations Using Lattice Gas Techniques

This paper originally appeared in *Los Alamos Science*, Special Issue, 1987, pages 201–210.

Over the last few years the tantalizing prospect of being able to perform hydrodynamic calculations orders-of-magnitude faster than present methods allow has prompted considerable interest in lattice gas techniques. A few dozen published papers have presented both advantages and disadvantages, and several groups have studied the possibilities of building computers specially designed for lattice gas calculations. Yet the hydrodynamics community remains generally skeptical toward this new approach. The question is often asked, "What calculations can be done with lattice gas techniques?" Enthusiasts respond that in principle the techniques are applicable to any calculation, adding cautiously that increased accuracy requires increased computational effort. Indeed, by adding more particle directions, more particles per site, more particle speeds, and more variety in the interparticle scattering rules, lattice gas methods can be tailored to achieve better and better accuracy. So the real problem is one of tradeoff: How much accuracy is gained by making lattice gas methods more complex, and what is the computational price of those complications? That problem has not yet been well studied. This paper and most of the research to date focus on the

simplest lattice gas models in the hope that knowledge of them will give some insight into the essential issues.

We begin by examining a few of the features of the simple models. We then display results of some calculations. Finally, we conclude with a discussion of limitations of the simple models.

FEATURES OF SIMPLE LATTICE GAS METHODS

We will discuss in some depth the memory efficiency and the parallelism of lattice gas methods, but first we will touch on their simplicity, stability, and ability to model complicated boundaries.

Computer codes for lattice gas methods are enormously simpler than those for other methods. Usually the essential parts of the code are contained in only a few dozen lines of FORTRAN. And those few lines of code are much less complicated than the several hundred lines of code normally required for two- and three-dimensional hydrodynamic calculations.

There are many hydrodynamic problems that cause most standard codes (such as finite-difference codes, spectral codes, and particle-in-cell codes) to crash. That is, the code simply stops running because the algorithm becomes unstable. Stability is not a problem with the codes for lattice gas methods. In addition, such methods conserve energy and momentum exactly, with no roundoff errors.

Boundary conditions are quite easy to implement for lattice gas methods, and they do not require much computer time. One simply chooses the cells to which boundary conditions apply and updates those cells in a slightly different way. One of three boundary conditions is commonly chosen: bounce-back, in which the directions of the reflected particles are simply reversed; specular, in which mirror-like reflection is simulated; or diffusive, in which the directions of the reflected particles are chosen randomly.

We consider next the memory efficiency of the lattice gas method. When the 2-dimensional hydrodynamic lattice gas algorithm is programmed on a computer with a word length of, say, 64 bits (such as the Cray X-MP), two impressive efficiencies occur. The first arises because every single bit of memory is used equally effectively. Coined "bit democracy" by von Neumann, such efficient use of memory should be contrasted with that attainable in standard calculations, where each number requires a whole 64-bit word. The lattice gas is "bit democratic" because all that one needs to know is whether or not a particle with a given velocity direction exists in a given cell. Since the number of possible velocity directions is six and no two particles in the same cell can have the same direction, only six bits of information are needed to completely specify the state of a cell. Each of those six bits corresponds to one of the six directions and is set to 1 if the cell contains a particle with that direction and to 0 otherwise. Suppose we designate the six directions by A, B, C, D, E, and F as shown in Figure 1. We associate each bit in the 64-bit word A with a different cell, say, the first 64 cells in the first row. If the first cell contains (does

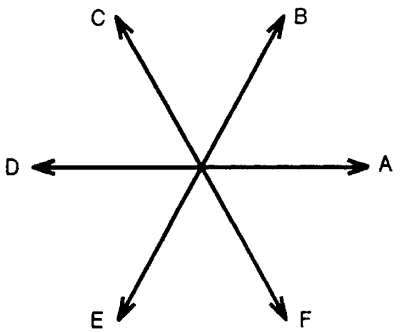

FIGURE 1 Six directions designated as A through F corresponding to six bits used to specify the state of a cell.

not contain) a particle with direction A, we set the first bit in A to 1 (0). Similarly, we pack information about particles in the remaining 63 cells with direction A into the remaining 63 bits of A. The same scheme is used for the other five directions. Consequently, all the information for the first 64 cells in the first row is contained in the six words,A, B, C, D, E, and F. Note that all bits are equally important and all are fully utilized.

To appreciate the significance of such efficient use of memory, consider how many cells can be specified in the solid-state storage device presently used with the Cray X-MP/416 at Los Alamos. That device stores 512,000,000 64-bit words. Since the necessary information for $10\frac{2}{3}$ cells can be stored in each word, the device can store information for about 5,000,000,000 cells, which corresponds to a two-dimensional lattice with 100,000 cells along one axis and 50,000 cells along the other. That number of cells is a few orders-of-magnitude greater than the number normally treated when other methods are used. (Although such high resolution may appear to be a significant advantage of the lattice gas method, some averaging over cells is required to obtain smooth results for physical quantities such as velocity and density.)

The second efficiency is related to the fact that lattice gas operations are bit oriented rather than floating-point-number oriented and therefore execute more naturally on a computer. Most computers can carry out logic operations bit by bit. For example, the result of the logic operation AND on the 64-bit words A and B is a new 64-bit word in which the ith bit has a value of 1 only if the ith bits of both A and B have values of 1. Hence in one clock cycle a logic operation can be performed on information for 64 cells. Since a Cray X-MP/416 includes eight logical function units, information for 8 times 64, or 512, cells can be processed during each clock cycle, which lasts about 10 nanoseconds. Thus information for 51,200,000,000 cells can be processed each second. The two-dimensional lattice gas models used so far require from about thirty to one hundred logic operations to implement the scattering rules and about another dozen to move the particles to the next cells. So the number of cells that can be updated each second by logic

operations is near 500,000,000. Cells can also be updated by table-look-up methods. The authors have a table-look-up code for three-dimensional hydrodynamics that processes about 30,000,000 cells per second.

A final feature of the lattice gas method is that the algorithm is inherently parallel. The rules for scattering particles within a cell depend only on the combination of particle directions in that cell. The scattering can be done by table look-up, in which one creates and uses a table of scattering results—one for each possible cell configuration. Or it can be done by logic operation.

USING LATTICE GAS METHODS TO APPROXIMATE HYDRODYNAMICS

In August 1985 Frisch, Hasslacher, and Pomeau demonstrated that one can approximate solutions to the Navier-Stokes equations by using lattice gas methods, but their demonstration applied only to low-velocity incompressible flows near equilibrium. No one knew whether more interesting flows could be approximated. Consequently, computer codes were written to determine the region of validity of the lattice gas method. Results of some of the first simulations done at Los Alamos and of some later simulations are shown in Figures 1 through 6. (Most of the early calculations were done on a Celerity computer, and the displays were done on a Sun workstation.) All the results indicate qualitatively correct fluid behavior.

Plate 1a (see color plates) demonstrates that a stable trailing vortex pattern develops in a 2-dimensional lattice gas flowing past a plate. Figure 1b shows that without a three-particle scattering rule, which removes the spurious conservation of momentum along each line of particles, no vortex develops.

Plate 2 shows that stable vortices develop in a lattice gas at the interface between fluids moving in opposite directions. The Kelvin-Helmholtz instability is known to initiate such vortices. The fact that lattice gas methods should stimulate vortex evolution was reassuring and caused several scientists to begin to study the new method.

Plate 3 shows the complicated wake that develops behind the V-shaped wedge in a uniform-velocity flow.

Plate 4 shows the periodic oscillation of a low-velocity wake behind a cylinder. With a Reynolds number of 76, the flow has a stable period of oscillation that slowly grows to its asymptotic limit.

Plate 5 shows a flow with a higher Reynolds number past an ellipse. The wake here becomes chaotic and quite sensitive to details of the flow.

Plate 6 shows views of a 3-dimensional flow around a square plate, which was one of the first results from Los Alamos in 3-dimensional lattice gas hydrodynamic simulations.

Rivet and Frisch and other French scientists have developed a similar code that measures the kinematic shear viscosity numerically; the results compare well with theoretical predictions.

The lattice gas calculations of a group at the University of Chicago (Kadanoff, McNamara, and Zanetti) for two-dimensional flow through a channel agree with the known parabolic velocity profile for low-velocity channel flows.

The above calculations, and many others, have established some confidence that qualitative features of hydrodynamic flows are simulated by lattice-gas methods. Problems encountered in detailed comparisons with other types of calculations are discussed in the next section.

LIMITATIONS OF SIMPLE LATTICE GAS MODELS

As we discussed earlier, lattice gas methods can be made more accurate by making them more complicated—by, for example, adding more velocity directions and magnitudes. But the added complications degrade the efficiency. We mention in this section some of the difficulties (associated with limited range of speed, velocity dependence of the equation of state, and noisy results) encountered in the simplest lattice-gas models.

The limited range of flow velocities is inherent in a model that assumes a single speed for all particles. The sound speed in such models can be shown to be about two-thirds of the particle speed. Hence flows in which the Mach number (flow speed divided by sound speed) is greater than 1.5 cannot be simulated. This difficulty is avoided by adding particles with a variety of speeds.

The limited range of velocities also restricts the allowed range of Reynolds numbers. For small Reynolds numbers (0 to 1000) the flow is smooth, for moderate Reynolds numbers (2000 to 6000) some turbulence is observed, and for high Reynolds numbers (10,000 to 10,000,000) extreme turbulence occurs. Since the effective viscosity, ν, is typically about 0.2 in two-dimensional problems, the Reynolds number scales with the characteristic length, l, allowed by computer memory. Currently the upper bound on l is of the order of 100,000.

The velocity dependence of the equation of state is unusual and is a consequence of the inherent Fermi-Dirac distribution of the lattice gas. The low-velocity equation of state for a lattice gas can be written as $p = \frac{1}{2}\rho\left(1 - \frac{1}{2}v^2\right)$, where p is the pressure, ρ is the density, and v is the flow speed. Thus, for constant-pressure flows, regions of higher velocity flows have higher densities.

The velocity dependence of the equation of state is related to the fact that lattice gas models lack Galilean invariance. The standard Navier-Stokes equation for incompressible fluids is

$$\frac{\partial v}{\partial t} + v \cdot \nabla v = -\nabla p + \nu \nabla^2 v.$$

But in the incompressible, low-velocity limit the single-speed hexagonal lattice gas follows the equation

$$\frac{\partial v}{\partial t} + g(\rho)v \cdot \nabla v = -\nabla p + \nu \nabla^2 v,$$

where

$$g(\rho) = \frac{3-\rho}{6-\rho}$$

and ρ is the average number of particles per cell. The extra factor $g(\rho)$ requires special treatment. The conventional way to adjust for the fact that $g(\rho)$ does not equal unity (as it does in the Navier-Stokes equation) is to simply scale the time, t, and the viscosity, ν, by the factor $g(\rho)$ as follows: $t' = g(\rho)t$ and $\nu' = \nu/g(\rho)$. (The pressure must also be scaled.) Hence a density-dependent scaling of the time, the viscosity, and the pressure is required to bring the lattice gas model into a form that closely approximates the hydrodynamics of incompressible fluids in the low-velocity limit.

Finally, the discreteness of the lattice gas approximation introduces noise into the results. One method of smoothing the results for comparison with other methods is to average in space and time. In practice, spatial averages are taken over 64, 256, 512, or 1024 neighboring cells for time-dependent flows in two dimensions. For steady-state flows, time averaging is done. The details of noise reduction are complicated, but they must be addressed in each comparison calculation. The presence of noise is both a virtue and a defect. Noise ensures that only robust (that is, physical) singularities survive, whereas in standard codes, which are subject to less noise, mathematical artifacts can produce singularities. On the other hand, the noise in the model can trigger instabilities.

CONCLUSION

In the last few years lattice gas methods have been shown to simulate the qualitative features of hydrodynamic flows in two and three dimensions. Precise comparisons with other methods of calculation remain to be done, but it is believed that the accuracy of the lattice gas method can be increased by making the models more complicated. But how complicated they have to be to obtain the desired accuracy is an unanswered question.

Calculations based on the simple models are extremely fast and can be made several orders-of-magnitude faster by using special-purpose computers, but the models must be extended to get quantitative results with an accuracy greater than 1 percent. Significant research remains to be done to determine the accuracy of a given lattice gas method for a given flow problem.

NOTE ADDED IN PROOF: Recently Kadanoff, McNamara, and Zanetti reported precise comparisons between theoretical predictions and lattice gas simulations. They used a seven-bit hexagonal model on a small automaton universe to simulate forced two-dimensional channel flow for long times. Three tests were used to probe the hydrodynamic and statistical-mechanical behavior of the model. The tests determined (1) the profile of momentum density in the channel, (2) the equation of state given by the statistical mechanics of the system, and (3) the logarithmic divergence in the viscosity (a famous effect in two-dimensional hydrodynamics and a deep test of the accuracy of the model in the strong nonlinear regime).

The results were impressive. First, to within the accuracy of the simulation, there is no discrepancy between the parabolic velocity profile predicted by macroscopic theory and the lattice gas simulation data. Second, the equation of state derived from theory fits the simulation data to better than 1 percent. Finally, the measured logarithmic divergence in the viscosity as a function of channel width agrees with prediction. These results are at least one order-of-magnitude more accurate than any previously reported calculations.

REFERENCES

1. University of Chicago, preprint, October 1987

U. Frisch†, B. Hasslacher‡, and Y. Pomeau*
†Centre National de la Recherche Scientifique, Observatoire de Nice, 06003 Nice Cedex, France; ‡Theoretical Division and Center for Nonlinear Studies, Los Alamos National Laboratory, Los Alamos, New Mexico 87545; and *Centre National de la Recherche Scientifique, Ecole Normale Supérieure, 75231 Paris Cedex, France, and Service de Physique Théorique, Centre d'Etudes Nucléaires de Saclay, 91191 Gif-sur-Yvette, France

Lattice-Gas Automata for the Navier-Stokes Equation

This paper originally appeared in *Physical Review Letters*, Volume 56, Number 14, April 7, 1986, pp. 1505–1508.

We show that a class of deterministic lattice gases with discrete Boolean elements simulates the Navier-Stokes equation, and can be used to design simple, massively parallel computing machines.

The relatively recent availability of sophisticated interactive digital simulation has led to considerable progress in the unraveling of universal features of complexity generated by nonlinear dynamical systems with few degrees of freedom. In contrast, nonlinear systems with many degrees of freedom, e.g., high-Reynolds-number flow, are understood only on a quite superficial level,[1] and are likely to remain so, unless they can be explored in depth, e.g., by interactive simulation. This is many orders of magnitude beyond the capacity of existing computational resources. There are similar limitations on our ability to simulate many other multidimensional field theories.

Massively parallel architectures and algorithms are needed to avoid the ultimate computation limits of the speed of light and various solid-state constraints. Also, when parameter space must be explored quickly and extreme accuracy is unnecessary, a floating-point representation may not be efficient. For example, to

compute the drag due to turbulent flow past an obstacle with a modest accuracy of 5 bits, common experience in computational fluid dynamics shows that intermediate computations require from 32 to 64 bits. Floating-point representations hierarchically favor bits in the most significant places,[2] which is a major cause of numerical instability. In principle, schemes which give bits equal weight would be preferable. Because of roundoff noise, a floating-point calculation can run away to unphysical regimes, in an attempt to treat each bit equally.

A simulation strategy can be devised which both is naturally parallel and treats all bits on an equal footing, for systems which evolve by discrete cellular automaton rules, with only local interactions.[3] This avoids the complex switching networks which limit the computational power of conventional parallel arrays.

There has been speculation that various physically interesting field equations can be approximated by the large-scale behavior of suitably chosen cellular automata.[4] We shall here construct lattice-gas automata which asymptotically go over to the incompressible 2-D and 3-D Navier-Stokes equations.

To understand the physics behind lattice gases, we first point out that a fluid can be described on three levels: the molecular level at which motion, usually Hamiltonian, is reversible; the kinetic level, in the irreversible low-density Boltzmann approximation; and the macroscopic level, in the continuum approximation. At the first two levels of description, the fluid is near thermodynamic equilibrium. In the last there are free thermodynamic variables: local density, momentum, temperature, etc. A macroscopic description of the fluid comes about by a patching together of equilibria which are varying slowly in space and time, implying continuum equations for thermodynamic variables as consistency conditions. This was first realized by Maxwell,[5] and put in final form by Chapman and Enskog.[6]

There are many ways of building microscopic models that lead to a given set of continuum equations. It is known that one can build two- and three-dimensional Boltzmann models, with a small number of velocity vectors, which, in the continuum limit, reproduce quite accurately major fluid dynamical features (e.g., shock waves in a dilute gas, etc.[7]). Such Boltzmann models are fundamentally probabilistic, discrete only in velocity, but continuous in space and time. In contrast, we will use lattice-gas models, which have a completely discrete phase space and time and therefore may be viewed as made of "Boolean molecules."

The simplest case is the Hardy, de Pazzis, and Pomeau model[8] (hereafter called HPP) which has an underlying regular, square, two-dimensional lattice with unit link lengths. At each vertex, there are up to four molecules of equal mass, with unit speed, whose velocities point in one of the four link directions. The simultaneous occupation of a vertex by identical molecules is forbidden. Time is also discrete. The update is as follows. First, each molecule moves one link, to the nearest vertex to which its velocity was pointing. Then, any configuration of exactly two molecules moving in opposite directions at a vertex (head-on collisions) is replaced by another one at right angles to the original. All other configurations are left unchanged. The HPP model has a number of important properties.[8] The crucial one is the existence of thermodynamic equilibria. No ergodic theorem is known, but relaxation

to equilibrium has been demonstrated numerically.[8] These equilibria have free *continuous* parameters, namely, the average density and momentum. The equilibrium distribution functions are completely factorized over vertices and directions, being independent of vertex position, but dependent on direction, unless the mean momentum vanishes. When the density and momentum are varied slowly in space and time, "macrodynamical" equations emerge which differ from the nonlinear Navier-Stokes equations in three respects.

The discrepancies may be classified as (1) lack of Galilean invariance, (2) lack of isotropy, and (3) a crossover dimension problem. Galilean invariance is by definition broken by the lattice; consequently, thermodynamic equilibria with different velocities cannot be related by a simple transformation. This is reflected by the nonlinear term in the momentum equation, containing a momentum flux tensor, which not only has quadratic terms in the hydrodynamic velocity $\mathbf{u}$, as it should be in the Navier-Stokes equation, but also has nonlinear corrections to arbitrarily high order in the velocity. However, these terms are negligible at low Mach number, a condition which also guarantees incompressibility. The HPP automaton is invariant under $\pi/2$ rotations. Such a lattice symmetry is insufficient to insure the isotropy of the fourth-degree tensor relating momentum flux to quadratic terms in the velocity. Finally, crossover dimension is a general property of two-dimensional hydrodynamics, when thermal noise is added to the Navier-Stokes equation or to the HPP version of it. Simply put, the viscosity develops a logarithmic scale dependence, which is a dimensional crossover phenomenon, common in phase transitions and field theory.[9] In three dimensions, this difficulty does not exist.

Focusing on the isotropy problem, we note that for the HPP model, the momentum flux tensor has the form

$$P_{\alpha\beta} = p\delta_{\alpha\beta} + T_{\alpha\beta\gamma\epsilon}u_\gamma u_\epsilon + O(u^4). \tag{1}$$

Here $p = \rho/2$ is the pressure; terms odd in $\mathbf{u}$ vanish by parity. The tensor T is, by construction, pairwise symmetric in both (α, β) and (γ, ϵ). Observe that when the underlying microworld is *two-dimensional* and invariant under the hexagonal rotation group (multiples of $\pi/3$), the tensor T is isotropic and Eq. (1) takes the form

$$P_{\alpha\beta} = (p + \mu u^2)\delta_{\alpha\beta} + \lambda u_\alpha u_\beta + O(u^4), \tag{2}$$

with suitable scalar factors λ and μ. At low Mach number, this is the correct form for the Navier-Stokes equation. This observation appears to be new. So, in two dimensions, we will use a triangular instead of a square lattice. Each vertex then has a hexagonal neighborhood (Figure 1). We will call this model the hexagonal lattice gas (HLG). The setup is the same as in the HPP lattice gas, except for modified collision rules. A suitable set is one given by Harris,[10] in connection with a discrete Boltzmann model, supplemented by a Fermi exclusion condition, of single occupation of each Boolean state. The Fermi-modified Harris rules are as follows: Number the six links out of any vertex counterclockwise, with an index i, defined on the integers (mod6). There are both two- and three-body collisions. For two-body

collisions, we have $(i, i+3)$ goes to (a) $(i+1, i-2)$ or (b) $(i-1, i+2)$. Type a and b outcomes have equal *a priori* weights. For three-body collisions we have $(i, i+2, i-2)$ goes to $(i+3, i+1, i-1)$. In these rules, it is assumed that no incident link to a vertex is populated, other than the ones given as initial states. All other configurations remain unaffected by collisions. These rules are designed to conserve particle number and momentum at each vertex, i.e., a total of three scalar conservation relations. Without three-body collisions, there would be four scalar conservation relations, namely mass and momentum along each of the three lattice directions.

Note that the HPP rules are invariant under duality (interchange of particles and holes), whereas the present rules are not. Duality can be restored by addition of suitable four-particle collision rules, but we will not use them here.

We display a variant of this model where at most one particle is allowed to remain at rest at each vertex. The rest particles are labeled by an asterisk and the previous rules are supplemented with $(i, i+2)$ goes to $(i-2, *)$ and $(i, *)$ goes to $(i+2, i-2)$. Additional variations on the model allow one to define a nontrivial temperature. The remainder of this discussion is concerned only with the basic (HLG) model.

We briefly outline how the hexagonal lattice gas leads to the two-dimensional Navier-Stokes equations. A detailed derivation will be presented elsewhere.[11] Let N_i be the average population at a vertex with velocity in the direction i. The average

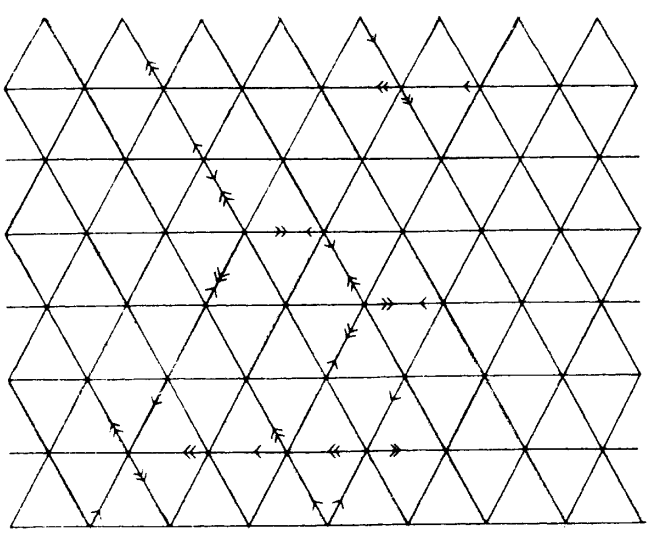

FIGURE 1 Triangular lattice with hexagonal symmetry and hexagonal lattice-gas rules. Particles at time t and $t+1$ are marked by single and double arrows, respectively.

is over a macroscopic space-time region so that N_i depends slowly on space and time variables. We define a slowly varying density ρ and momentum $\rho\mathbf{u}$ by

$$\rho = \sum_i N_i, \qquad \rho\mathbf{u} = \sum_i N_i \mathbf{c}_i, \tag{3}$$

where $\mathbf{c}_i$ is a unit vector in the direction i. Locally, for a given ρ and $\mathbf{u}$, the N_i's can be computed from both these definitions and the detailed-balance equations at thermodynamic equilibrium, which are too involved to present here. This gives a Fermi-Dirac distribution:

$$N_i = \left\{1 + \exp\left[\alpha(\rho, u) + \beta(\rho, u)\mathbf{c}_i \cdot \mathbf{u}\right]\right\}^{-1}. \tag{4}$$

In general, α and β satisfy equations with no simple solutions. However, when $\mathbf{u} = 0$, it is obvious by symmetry that $N_i = \rho/6$. Therefore, α and β can be expanded in a Taylor series around $\mathbf{u} = 0$. The result can be used to compute mass and momentum flux to first order in the macroscopic gradients. Second-order terms in the gradients (viscous terms) are obtained by Green-Kubo relations or by a Chapman-Enskog expansion.[12] The following set of hydrodynamic equations is thus obtained:

$$\frac{\partial \rho}{\partial t} + \nabla \cdot (\rho \mathbf{u}) = 0, \tag{5}$$

$$\frac{\partial}{\partial t}(\rho u_\alpha) + \sum_\beta \frac{\partial}{\partial x_\beta}\left[g(\rho)\rho u_\alpha u_\beta + O(u^4)\right] = -\frac{\partial}{\partial x_\alpha} p + \eta_1(\rho)\nabla^2 u_\alpha + \eta_2(\rho)\frac{\partial}{\partial x_\alpha}\nabla \cdot \mathbf{u}, \tag{6}$$

with $g(\rho) = (\rho - 3)/(\rho - 6)$ and $p = \rho/2$. $\eta_1(\rho)$ and $\eta_2(\rho)$ are the shear and bulk viscosities.[12] Deletion of the nonlinear and viscous terms gives the wave equation for sound waves propagating isotropically with a speed equal to the "velocity of light" (here set equal to 1) over $\sqrt{2}$, just as for a two-dimensional photon gas. These sound waves have been observed in simulations on the MIT cellular automaton machine by Margolus, Toffoli, and Vichniac.[13] They used lattice-gas models that yield the same wave equation as above.

The nonlinear system (5) and (6) goes over to the incompressible Navier-Stokes equation by the following limiting procedure: Let the Mach number $M = u\sqrt{2}$ tend to zero, and the hydrodynamic scale L tend to infinity, while keeping their product fixed. As in the usual derivation of the incompressible limit, density fluctuations become irrelevant, except in the pressure term; also, the continuity equation (5) reduces to $\nabla \cdot \mathbf{u} = 0$. Thus, the factor $g(\rho)$ is to leading order a constant and may, for $0 < \rho < 3$, be absorbed in a rescaled time. The resulting Reynolds number is

$$N_R = \frac{ML\rho g(\rho)}{\sqrt{2}\eta_1(\rho)}. \tag{7}$$

Note that Galilean invariance, which does not hold at the lattice level, is restored macroscopically.

A straightforward lift of the hexagonal lattice-gas model from two into three dimensions does not work. The reason is that the regular space-filling simplex with the greatest symmetry in three dimensions is the face centered cubic, with twelve equal-speed velocity directions out of each vertex. Unfortunately, the relevant tensors such as $T_{\alpha\beta\gamma\epsilon}$ in Eq. (1) depend now on three constants. This induces a spurious, isotropy-breaking term in the Navier-Stokes equation, proportional to $(\partial/\partial x_\alpha)u_\alpha^2$ (no summation on α).

This obstacle may be removed by a splitting method. The nonlinear term in the three-dimensional Navier-Stokes equation is recast as the sum of two terms, each containing spurious elements and each realizable on a different lattice (for example, a face-centered-cubic lattice and a regular cubic lattice).

In lattice-gas models, as in general cellular automata (CA's), boundary conditions are very easy to implement. Specular reflection of molecules gives so-called "free slip" boundary conditions for the hydrodynamic velocity $\mathbf{u}$. "Rigid" boundary conditions are obtained either by random scattering of particles back into the incoming half plane from a locally planar boundary, or by specular reflection from a microscale roughened version of the macroscopic boundary.

We mention some practical limitations on lattice-gas models. For the hydrodynamic description to hold, there must be a scale separation between the smallest hydrodynamic scale and the lattice link length; as we shall see, this requirement is automatically satisfied. Lattice-gas models must be run at moderate Mach numbers M (say, 0.3 to 0.5), to remain incompressible, and to avoid spurious high-order nonlinear terms. For fixed Mach numbers, the largest Reynolds number associated with a D-dimensional lattice with $O(N)$ sites in each direction is $O(N)$. This is because in our units, the kinematic viscosity of the hexagonal lattice gas is $O(1)$. From standard turbulence theory,[14] it follows that the dissipation scale is $O(N^{1/2})$ in 2D and $O(N^{1/4})$ in 3D. This insures the required scale separation at large Reynolds numbers. It would, however, be desirable to reduce the scale separation, especially in 2D, to avoid excessive storage requirements compared to conventional incompressible floating-point simulations (in the latter, the mesh can be taken comparable to the dissipation scale).

For this, we observe that the viscosity in the lattice gas is decreased by a factor P if we subdivide each cell into a sublattice with links P times smaller. We note also that the sublattice need not be similar to the original lattice. It must have the same collision rules, to preserve local thermodynamic equilibria, but the geometry does not matter since macroscopic quantities may be considered uniform over the cell. Thus, all the sublattice vertices in a given cell may be regarded as indistinguishable and can be coded in $O(\ln P)$ rather than $O(P^D)$ bits; interactions occur between randomly chosen vertex pairs within cells and between neighboring cells, the latter being less frequent by a factor $O(1/P)$.

Simulations of the models discussed here, done on general-purpose computers and exhibiting a variety of known two-dimensional hydrodynamic phenomena, have been made by d'Humières, Lallemand, and Shimomura.[15]

We have given a concrete hydrodynamical example of how CA's can be used to simulate classical nonlinear fields. We expect that further CA implementations will be found for the Navier-Stokes equation and other problems, not necessarily based on thermalized lattice gases and possibly less constrained than ours.

S. Wolfram stimulated our interest in cellular automata as a possible new approach to turbulence phenomena. Acknowledgments are also due to T. Bloch, R. Caflish, D. d'Humières, R. Gatignol, R. Kraichnan, P. Lallemand, N. Margolus, D. Nelson, J. L. Oneto, S. A. Orszag, J. P. Rivet, T. Shimomura, Z. S. She, B. Shraiman, T. Toffoli, and G. Vichniac, as well as the following: Woods Hole Geophysical Fluid Dynamics Summer Program (U.F., Y.P.); Aspen Center for Physics, 1985 Chaos Workshop (B.H.); and Service de Physique Théorique, Centre d'Etudes Nucleaires de Saclay (B.H.). This work was supported in part by National Science Foundation Grant No. 8442384.

REFERENCES

1. Frisch, U. *Phys. Scr.* **T9** (1985):131.
2. Knuth, D. E. *The Art of Computer Programming: Semi-Numerical Algorithms*, vol. 2. Reading, MA: Addison-Wesley, 1981, 238.
3. Toffoli, T. *Physica* (Amsterdam) **10D** (1984):117; Wolfram, S. *Nature* **311** (1984):419.
4. Pomeau, Y. *J. Phys. A* **17** (1984):L415; Vichniac, G. *Physica* (Amsterdam) **10D** (1984):96, and references therein; Margolus, N. *Physica* (Amsterdam) **10D** (1984):81.
5. Maxwell, J. C. *The Scientific Papers*, vol. 2. Cambridge, England: Cambridge Univ. Press, 1890, 681.
6. Uhlenbeck, G. E., and G. W. Ford. "Lectures in Statistical Mechanics." *Lectures in Applied Math.*, vol. 1. Providence, RI: American Mathematical Society, 1963.
7. Broadwell, J. E. *Phys. Fluids* **7** (1964):1243; Gatignol, R. "Théorie Cinétique des Gaz à Répartition Discrète des Vitesses." *Lecture Notes in Physics*, vol. 36. Berlin: Springer, 1964.
8. Hardy, J., and Y. Pomeau. *J. Math. Phys.* **13** (1972):1042; Hardy, J., Y. Pomeau, and O. de Pazzis. *J. Math. Phys.* **14** (1973):1746; Hardy, J., O. de Pazzis, and Y. Pomeau. *Phys. Rev. A* **13** (1976):1949.
9. Forster, D., D. R. Nelson, and M. J. Stephen. *Phys. Rev. A.* **16** (1977):732.
10. Harris, S. *Phys. Fluids* 9 (1966):1328.
11. Frisch, U., D. d'Humières, B. Hasslacher, P. Lallemand, Y. Pomeau, and J.-P. Rivet. "Lattice Gas Hydrodynaamics in Two and Three Dimensions." Reprinted in this volume.
12. Rivet, J., and U. Frisch. *C.R. Seances Acad. Sci., Ser. 2* **302** (1986):267.
13. Margolus, N., T. Toffoli, and G. Vichniac. Private communication; *Massachusetts Institute of Technology Technical Memo No. LCS-TM-296*, 1984.
14. Kolmogorov, A. N. *C.R. (Dokl.) Acad. Sci. USSR* **30** (1941):301, 538; Kraichnan, R. *Phys. Fluids* **10** (1967):1417; Batchelor, G. K. *Phys. Fluids* **12**, Suppl. 2 (1969):233.
15. d'Humières, D., P. Lallemand, and T. Shimomura. "Lattice Gas Cellular Automata, A New Experimental Tool for Hydrodynamics," to be published.

Stephen Wolfram
The Institute for Advanced Study, Princeton, New Jersey and Thinking Machines Corporation, 245 First Street, Cambridge, Massachusetts 02142; present address Center for Complex Systems Research, and Departments of Physics, Mathematics and Computer Science, University of Illinois, 508 South Sixth Street, Champaign, Illinois 61820

Cellular Automaton Fluids 1: Basic Theory

This paper originally appeared in the *Journal of Statistical Physics*, volume 45, nos. 3/4 (1986), pp. 471–526.

Continuum equations are derived for the large-scale behavior of a class of cellular automaton models for fluids. The cellular automata are discrete analogues of molecular dynamics, in which particles with discrete velocities populate the links of a fixed array of sites. Kinetic equations for microscopic particle distributions are constructed. Hydrodynamic equations are then derived using the Chapman-Enskog expansion. Slightly modified Navier-Stokes equations are obtained in two and three dimensions with certain lattices. Viscosities and other transport coefficients are calculated using the Boltzmann transport equation approximation. Some corrections to the equations of motion for cellular automaton fluids beyond the Navier-Stokes order are given.

Key words: Cellular automata; derivation of hydrodynamics; molecular dynamics; kinetic theory; Navier-Stokes equations.

Lattice Gas Methods for Partial Differential Equations, SFI SISOC,
Eds. Doolen et al., Addison-Wesley Publishing Group Ltd., 1990

1. INTRODUCTION

Cellular automata (e.g., Refs. 1 and 2) are arrays of discrete cells with discrete values. Yet sufficiently large cellular automata often show seemingly continuous macroscopic behavior (e.g., Refs. 1 and 3). They can thus potentially serve as models for continuum systems, such as fluids. Their underlying discreteness, however, makes them particularly suitable for digital computer simulation and for certain forms of mathematical analysis.

On a microscopic level, physical fluids consist of discrete particles. But on a large scale, they, too, seem continuous, and can be described by the partial differential equations of hydrodynamics (e.g., Ref. 4). The form of these equations is in fact quite insensitive to microscopic details. Changes in molecular interaction laws can affect parameters such as viscosity, but do not alter the basic form of the macroscopic equations. As a result, the overall behavior of fluids can be found without accurately reproducing the details of microscopic molecular dynamics.

This paper is the first in a series which considers models of fluids based on cellular automata whose microscopic rules give discrete approximations to molecular dynamics.[1] The paper uses methods from kinetic theory to show that the macroscopic behavior of certain cellular automata corresponds to the standard Navier-Stokes equations for fluid flow. The next paper in the series[16] describes computer experiments on such cellular automata, including simulations of hydrodynamic phenomena.

Figure 1 shows an example of the structure of a cellular automaton fluid model. Cells in an array are connected by links carrying a bounded number of discrete "particles." The particles move in steps and "scatter" according to a fixed set of deterministic rules. In most cases, the rules are chosen so that quantities such as particle number and momentum are conserved in each collision. Macroscopic variations of such conserved quantities can then be described by continuum equations.

Particle configurations on a microscopic scale are rapidly randomized by collisions, so that a local equilibrium is attained, described by a few statistical average quantities. (The details of this process will be discussed in a later paper.) A master equation can then be constructed to describe the evolution of average particle densities as a result of motion and collisions. Assuming slow variations with position and time, one can then write these particle densities as an expansion in terms of macroscopic quantities such as momentum density. The evolution of these quantities is determined by the original master equation. To the appropriate order in the

[1]This work has many precursors. A discrete model of exactly the kind considered here was discussed in Ref. 6. A version on a hexagonal lattice was introduced in Ref. 7, and further studied in Refs. 8,9. Related models in which particles have a discrete set of possible velocities, but can have continuously variable positions and densities, were considered much earlier.[10,14] Detailed derivations of hydrodynamic behavior do not, however, appear to have been given even in these cases (see, however, e.g., Ref. 15).

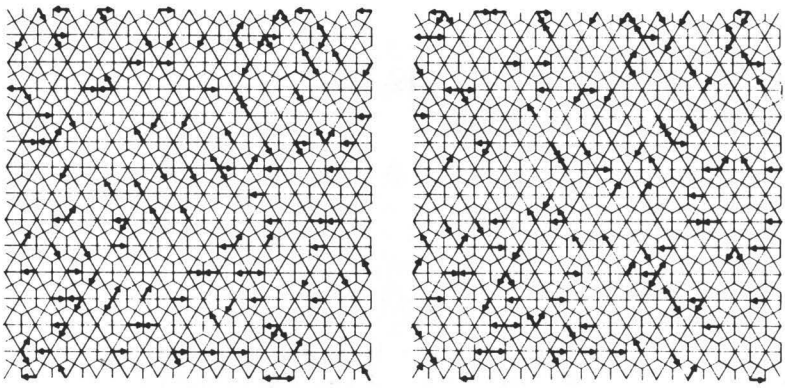

FIGURE 1 Two successive microscopic configurations in the typical cellular automaton fluid model discussed in Section 2. Each arrow represents a discrete "particle" on a link of the hexagonal grid. Continuum behavior is obtained from averages over large numbers of particles.

expansion, certain cellular automaton models yield exactly the usual Navier-Stokes equations for hydrodynamics.

The form of such macroscopic equations is in fact largely determined simply by symmetry properties of the underlying cellular automaton. Thus, for example, the structure of the nonlinear and viscous terms in the Navier-Stokes equations depends on the possible rank three and four tensors allowed by the symmetry of the cellular automaton array. In two dimensions, a square lattice of particle velocities gives anisotropic forms for these terms.[6] A hexagonal lattice, however, has sufficient symmetry to ensure isotropy.[7] In three dimensions, icosahedral symmetry would guarantee isotropy, but no crystallographic lattice with such a high degree of symmetry exists. Various structures involving links beyond nearest neighbors on the lattice can instead be used.

Although the overall form of the macroscopic equations can be established by quite general arguments, the specific coefficients which appear in them depend on details of the underlying model. In most cases, such transport coefficients are found from explicit simulations. But, by using a Boltzmann approximation to the master equation, it is possible to obtain some exact results for such coefficients, potentially valid in the low-density limit.

This paper is organized as follows. Section 2 describes the derivation of kinetic and hydrodynamic equations for a particular sample cellular automaton fluid model. Section 3 generalizes these results and discusses the basic symmetry conditions necessary to obtain standard hydrodynamic behavior. Section 4 then uses the Boltzmann equation approximation to investigate microscopic behavior and obtain results for transport coefficients. Section 5 discusses a few extensions of the model. The Appendix gives an SMP program[17] used to find macroscopic equations for cellular automaton fluids.

2. MACROSCOPIC EQUATIONS FOR A SAMPLE MODEL

2.1. STRUCTURE OF THE MODEL

The model[7] is based on a regular two-dimensional lattice of hexagonal cells, as illustrated in Figure 1. The site at the center of each cell is connected to its six neighbors by links corresponding to the unit vectors $\mathbf{e}_1$ through $\mathbf{e}_6$ given by

$$\mathbf{e}_a = \left(\cos(2\pi a/6), \sin(w\pi a/6)\right). \tag{2.1.1}$$

At each time step, zero or one particle lie on each directed link. Assuming unit time steps and unit particle masses, the velocity and momentum of each particle is given simply by its link vector $\mathbf{e}_a$. In this model, therefore, all particles have equal kinetic energy, and have zero potential energy.

The configuration of particles evolves in a sequence of discrete time steps. At each step, every particle first moves by a displacement equal to its velocity $\mathbf{e}_a$. Then the particles on the six links at each site are rearranged according to a definite set of rules. The rules are chosen to conserve the number and total momentum of the particles. In a typical case, pairs of particles meeting head on might scatter through 60°, as would triples of particles 120° apart. The rules may also rearrange other configurations, such as triples of particles meeting asymmetrically. Such features are important in determining parameters such as viscosity, but do not affect the form of the macroscopic equations derived in this section.

To imitate standard physical processes, the collision rules are usually chosen to be microscopically reversible. There is therefore a unique predecessor, as well as a unique successor, for each microscopic particle configuration. The rules for collisions in each cell thus correspond to a simple permutation of the possible particle arrangements. Often the rules are self-inverse. But, in any case, the evolution of a complete particle configuration can be reversed by applying inverse collision rules at each site.

The discrete nature of the cellular automaton model makes such precise reversal in principle possible. But the rapid randomization of microscopic particle configurations implies that very complete knowledge of the current configuration is needed. With only partial information, the evolution may be effectively irreversible.[8,19]

2.2. BASIS FOR KINETIC THEORY

Cellular automaton rules specify the precise deterministic evolution of microscopic configurations. But if continuum behavior is seen, an approximate macroscopic description must also be possible. Such a description will typically be a statistical one, specifying not, for example, the exact configuration of particles, but merely the probabilities with which different configurations appear.

A common approach is to consider ensembles in which each possible microscopic configuration occurs with a particular probability (e.g., Ref. 18). The reversibility of the microscopic dynamics ensures that the total probability for all configurations

in the ensemble must remain constant with time. The probabilities for individual configurations may, however, change, as described formally by the Liouville equation.

An ensemble is in "equilibrium" if the probabilities for configurations in it do not change with time. This is the case for an ensemble in which all possible configurations occur with equal probability. For cellular automata with collision rules that conserve momentum and particle number, the subsets of this ensemble that contain only those configurations with particular total values of the conserved quantities also correspond to equilibrium ensembles.

If the collision rules effectively conserved absolutely no other quantities, then momentum and particle number would uniquely specify an equilibrium ensemble. This would be the case if the system were ergodic, so that starting from any initial configuration, the system would eventually visit all other microscopic configurations with the same values of the conserved quantities. The time required would, however, inevitably be exponentially long, making this largely irrelevant for practical purposes.

A more useful criterion is that starting from a wide range of initial ensembles, the system evolves rapidly to ensembles whose statistical properties are determined solely from the values of conserved quantities. In this case, one could assume for statistical purposes that the ensemble reached contains all configurations with these values of the conserved quantities, and that the configurations occur with equal probabilities. This assumption then allows for the immediate construction of kinetic equations that give the average rates for processes in the cellular automaton.

The actual evolution of a cellular automaton does not involve an ensemble of configurations, but rather a single, specific configuration. Statistical results may nevertheless be applicable if the behavior of this single configuration is in some sense "typical" of the ensemble.

This phenomenon is in fact the basis for statistical mechanics in many different systems. One assumes that appropriate space or time averages of an individual configuration agree with averages obtained from an ensemble of different configurations. This assumption has never been firmly established in most practical cases; cellular automata may in fact be some of the clearest systems in which to investigate it.

The assumption relies on the rapid randomization of microscopic configurations, and is closely related to the second law of thermodynamics. At least when statistical or coarse-grained measurements are made, configurations must seem progressively more random, and must, for example, show increasing entropies. Initially ordered configurations must evolve to apparent disorder.

The reversibility of the microscopic dynamics nevertheless implies that ordered initial configurations can always in principle be reconstructed from a complete knowledge of these apparently disordered states. But just as in pseudorandom sequence generators or cryptographic systems, the evolution may correspond to a sufficiently complex transformation that any regularities in the initial conditions cannot readily be discerned. One suspects in fact that no feasibility simple computation can discover such regularities from typical coarse-grained measurements.[19,20]

As a result, the configurations of the system seem random, at least with respect to standard statistical procedures.

While most configurations may show progressive randomization, some special configurations may evolve quite differently. Configurations obtained by computing time-reversed evolution from ordered states will, for example, evolve back to ordered states. Nevertheless, one suspects that the systematic construction of such "antithermodynamic" states must again require detailed computations of a complexity beyond that corresponding to standard macroscopic experimental arrangements.

Randomization requires that no additional conserved quantities are present. For some simple choices of collision rules, spurious conservation laws can nevertheless be present, as discussed in Section 4.5. For most of the collision rules considered in this paper, however, rapid microscopic randomization does seem to occur.

As a result, one may use a statistical ensemble description. Equilibrium ensembles in which no statistical correlations are present should provide adequate approximations for many macroscopic properties. At a microscopic level, however, the deterministic dynamics does lead to correlations in the detailed configurations of particles.[2] Such correlations are crucial in determining local properties of the system. Different levels of approximation to macroscopic behavior are obtained by ignoring correlations of different orders.

Transport and hydrodynamic phenomena involve systems whose properties are not uniform in space and time. The uniform equilibrium ensembles discussed above cannot provide exact descriptions of such systems. Nevertheless, so long as macroscopic properties vary slowly enough, collisions should maintain approximate local equilibrium, and should make approximations based on such ensembles accurate.

2.3. KINETIC EQUATIONS

An ensemble of microscopic particle configurations can be described by a phase space distribution function which gives the probability for each complete configuration. In studying macroscopic phenomena, it is, however, convenient to consider reduced distribution functions, in which an average has been taken over most degrees of freedom in the system. Thus, for example, the one-particle distribution function $f_a(\mathbf{x},t)$ gives the probability of finding a particle with velocity $\mathbf{e}_a$ at position $\mathbf{x}$ and time t, averaged over all other features of the configuration (e.g., Ref. 23).

Two processes lead to changes in f_a with time: motion of particles from one cell to another, and interactions between particles in a given cell. A master equation can be constructed to describe these processes.

[2]The kinetic theory approach used in this paper concentrates on average particle distribution functions. An alternative but essentially equivalent approach concentrates on microscopic correlation functions (e.g., Refs. 21, 22).

In the absence of collisions, the cellular automaton rules imply that all particles in a cell at position $\mathbf{X}$ with velocity $\mathbf{e}_a$ move at the next time step to the adjacent cell at position $\mathbf{X}+\mathbf{e}_a$. As a result, the distribution function evolves according to

$$f_a(\mathbf{X}+\mathbf{e}_a, T+1) = f_a(\mathbf{X}, T)\,. \tag{2.3.1}$$

For large lattices and long time intervals, position and time may be approximated by continuous variables. One may define, for example, scaled variables $\mathbf{x} = \delta_x \mathbf{X}$ and $t = \delta_t T$, where $\delta_x,\ \delta_t \ll 1$. In terms of these scales variables, the difference equation (2.3.1) becomes

$$f_a(\mathbf{x}+\mathbf{e}_a\delta_x, t+\delta_t) - f_a(\mathbf{x}, t) = 0\,. \tag{2.3.2}$$

In deriving macroscopic transport equations, this must be converted to a differential equation. Carrying out a Taylor expansion, one obtains[24]

$$\delta_t\partial_t f_a + \delta_x \mathbf{e}_a\cdot\nabla f_a + \frac{1}{2}\delta_t^2\partial_{tt} f_a + \delta_x\delta_t(\mathbf{e}_a\cdot\nabla)\partial_t f_a + \frac{1}{2}\delta_x^2(\mathbf{e}_a\cdot\nabla)^2 f_a + O(\delta^3) = 0. \tag{2.3.3}$$

If all variations in the f_a are assumed small, and certainly less than $O(1/\delta_x, 1/\delta_t)$, it suffices to keep only first-order terms in δ_x, δ_t. In this way one obtains the basic transport equation

$$\partial_t f_a(\mathbf{x}, t) + \mathbf{e}_a\cdot\nabla f_a(\mathbf{x}, t) = 0\,. \tag{2.3.4}$$

This has the form of a collisionless Boltzmann transport equation for f_a (e.g., Ref. 25). It implies, as expected, that f_a is unaffected by particle motion in a spatially uniform system.

Collisions can, however, change f_a even in a uniform system, and their effect can be complicated. Consider, for example, collisions that cause particles in directions $\mathbf{e}_1$ and $\mathbf{e}_4$ to scatter in directions $\mathbf{e}_2$ and $\mathbf{e}_5$. The rate for such collisions is determined by the probability that particles in directions $\mathbf{e}_1$ and $\mathbf{e}_4$ occur together in a particular cell. This probability is defined as the joint two-particle distribution function $\tilde{F}_{14}^{(2)}$. The collisions deplete the population of particles in direction $\mathbf{e}_1$ at a rate $\tilde{F}_{14}^{(2)}$. Microscopic reversibility guarantees the existence of an inverse process, which increases the population of particles in direction $\mathbf{e}_1$ at a rate given in this case by $\tilde{F}_{25}^{(2)}$. Notice that in a model where there can be at most one particle on each link, the scattering to directions $\mathbf{e}_2$ and $\mathbf{e}_5$ in a particular cell can occur only if no particles are already present on these links. The distribution function $\tilde{F}$ is constructed to include this effect, which is mathematically analogous to the Pauli exclusion principle for fermions.

The details of collisions are, however, irrelevant to the derivation of macroscopic equations given in this section. As a result, the complete change due to collisions in a one-particle distribution function f_a will for now be summarized by a simple "collision term" Ω_a, which in general depends on two-particle and higher-order distribution functions. (In the models considered here, Ω_a is always entirely local,

and cannot depend directly on, for example, derivatives of distribution functions.) In terms of Ω_a, the kinetic equation (2.3.3) extended to include collisions becomes

$$\partial_t f_a + \mathbf{e}_a \cdot \nabla f_a = \Omega_a \,. \tag{2.3.5}$$

With the appropriate form for Ω_a, this is an exact statistical equations for f_a (at least to first order in δ).

But the equation is not in general sufficient to determine f_a. It gives the time evolution of f_a in terms of the two-particle and higher-order distribution functions that appear in Ω_a. The two-particle distribution function then in turn satisfies an equation involving three-particle and higher-order distribution functions, and so on. The result is the exact BBGKY hierarchy of equations,[23] of which Eq. (2.3.5) is the first level.

The Boltzmann transport equation approximates (2.3.5) by assuming that Ω_a depends only on one-particle distribution functions. In particular, one may make a "molecular chaos" assumption that all sets of particles are statistically uncorrelated before each collision, so that multiple-particle distribution functions can be written as products of one-particle ones. The distribution function $\tilde{F}^{(2)}_{14}$ is thus approximated as $f_1 f_4(1-f_2)(1-f_3)(1-f_5)(1-f_6)$. The resulting Boltzmann equations will be used in Section 4. In this section, only the general form (2.3.5) is needed.

The derivation of Eq. (2.3.5) has been discussed here in the context of a cellular automaton model in which particles are constrained to lie on the links of a fixed array. In this case, the maintenance of terms in (2.3.3) only to first order in δ_x, δ_t is an approximation, and corrections can arise, as discussed in Section 2.5.[24] Equation (2.3.5) is, however, exact for a slightly different class of models, in which particles have a discrete set of possible velocities, but follow continuous trajectories with arbitrary spatial positions. Such "discrete velocity gases" have often been considered, particularly in studies of highly rarefied fluids, in which the mean distance between collisions is comparable to the overall system size.[11,14]

2.4. CONSERVATION LAWS

The one-particle distribution functions typically determine macroscopic average quantities. In particular, the total particle density n is given by

$$\sum_a f_a = n \,. \tag{2.4.1}$$

while the momentum density $n\mathbf{u}$, where $\mathbf{u}$ is the average fluid velocity, is given by

$$\sum_a \mathbf{e}_a f_a = n\mathbf{u} \,. \tag{2.4.2}$$

The conservation of these quantities places important constraints on the behavior of the f_a.

In a uniform system $\nabla f_a = 0$, so that Eq. (2.3.5) becomes

$$\partial_t f_a = \Omega_a \tag{2.4.3}$$

and Eqs. (2.4.1) and (2.4.2) imply

$$\sum_a \Omega_a = 0\,, \tag{2.4.4}$$

$$\sum_a \mathbf{e}_a \Omega_a = 0\,. \tag{2.4.5}$$

Using the kinetic equation (2.3.5), Eq. (2.4.4) implies

$$\partial_t \sum_a f_a + \sum_a \mathbf{e}_a \cdot \nabla f_a = 0\,. \tag{2.4.6}$$

With the second term in the form $\nabla \cdot (\sum \mathbf{e}_a f_a)$, Eq. (2.4.6) can be written exactly in terms of macroscopic quantities as

$$\partial_t n + \nabla \cdot (n\mathbf{u}) = 0\,, \tag{2.4.7}$$

this is the usual continuity equation, which expresses the conservation of fluid. It is a first example of a macroscopic equation for the average behavior of a cellular automaton fluid.

Momentum conservation yields the slightly more complicated equation

$$\partial_t \sum_a \mathbf{e}_a f_a + \sum_a \mathbf{e}_a (\mathbf{e}_a \cdot \nabla f_a) = 0\,. \tag{2.4.8}$$

Defining the momentum flux density tensor

$$\Pi_{ij} = \sum_a (\mathbf{e}_a)_i (\mathbf{e}_a)_j f_a\,. \tag{2.4.9}$$

Eq. (2.4.8) becomes

$$\partial_t (n u_i) + \partial_j \Pi_{ij} = 0\,. \tag{2.4.10}$$

No simple macroscopic result for Π_{ij} can, however, be obtained directly from the definitions (2.4.1) and (2.4.2).

Equations (2.4.7) and (2.4.10) have been derived here from the basic transport equation (2.3.5). However, as discussed in Section 2.3, this transport equation is only an approximation, valid to first order in the lattice scale parameters δ_x, δ_t.[24] Higher-order versions of (2.4.7) and (2.4.10) may be derived from the original Taylor expansion (2.3.3), and in some cases, correction terms are obtained.[24]

Assuming $\delta_x = \delta_t = \delta$, Eq. (2.4.6) to second order becomes

$$\sum_a \left[(\partial_t + \mathbf{e}_a \cdot \nabla) + \frac{1}{2}\delta (\partial_t + \mathbf{e}_a \cdot \nabla)^2 \right] = 0\,. \tag{2.4.11}$$

Writing the $O(\delta)$ term in the form

$$\partial_t \sum_a (\partial_t + \mathbf{e}_a \cdot \nabla) f_a + \sum_a (\partial_t + \mathbf{e}_a \cdot \nabla) \mathbf{e}_a f_a \,, \tag{2.4.12}$$

this term is seen to vanish for any f_a that satisfies the first-order equations (2.4.7) and (2.4.10). Lattice discretization effects thus do not affect the continuity equation (2.4.7), at least to second order.

Corrections do, however, appear at this order in the momentum equation (2.4.10). To second order, Eq. (2.4.8) can be written as

$$\begin{aligned} &\sum_a (\partial_t + \mathbf{e}_a \cdot \nabla) \mathbf{e}_a f_a + \frac{1}{2}\delta \partial_t \sum_a (\partial_t + \mathbf{e}_a \cdot \nabla) \mathbf{e}_a f_a \\ &\quad + \frac{1}{2}\delta \sum_a \left[\mathbf{e}_a \cdot \nabla \partial_t + (\mathbf{e}_a \cdot \nabla)^2\right] \mathbf{e}_a f_a = 0. \end{aligned} \tag{2.4.13}$$

The second term vanishes if f_a satisfies the first-order equation (2.4.8). The third term, however, contains piece trilinear in the $\mathbf{e}_a$, which gives a correction to the momentum equation (2.4.10).[24]

2.5. CHAPMAN-ENSKOG EXPANSION

If there is local equilibrium, as discussed in Section 2.2., then the microscopic distribution functions $f_a(\mathbf{x}, t)$ should depend, on average, only on the macroscopic parameters $\mathbf{u}(\mathbf{x}, t)$ and $n(\mathbf{x}, t)$ and their derivatives. In general, this dependence may be very complicated. But in hydrodynamic processes, $\mathbf{u}$ and n vary only slowly with position and time. In addition, in the subsonic limit, $|\mathbf{u}| \ll 1$.

With these assumptions, one may approximate the f_a by a series or Chapman-Enskog expansion in the macroscopic variables. To the order required for standard hydrodynamic phenomena, the possible terms are

$$\begin{aligned} f_a = f\Big\{ &1 + c^{(1)} \mathbf{e}_a \cdot \mathbf{u} + c^{(2)} \left[(\mathbf{e}_a \cdot \mathbf{u})^2 - \frac{1}{2}|\mathbf{u}|^2\right] \\ &+ c_\nabla^{(2)} \left[(\mathbf{e}_a \cdot \nabla)(\mathbf{e}_a \cdot \mathbf{u}) - \frac{1}{2}\nabla \cdot \mathbf{u}\right] + \cdots \Big\} \end{aligned} \tag{2.5.1}$$

where the $c^{(i)}$ are undetermined coefficients. The first three terms here represent the change in microscopic particle densities as a consequence of changes in macroscopic fluid velocity; the fourth term accounts for first-order dependence of the particle densities on macroscopic spatial variations in the fluid velocity. The structures of these terms can be deduced merely from the need to form scalar quantities f_a from the vectors $\mathbf{e}_a$, $\mathbf{u}$ and ∇.

The relation

$$\sum_a (\mathbf{e}_a)_i (\mathbf{e}_a)_j = \frac{M}{d}\delta_{ij} \tag{2.5.2}$$

where here $M = 6$ and $d = 2$, and i and j are space indices, has been used in Eq. (2.5.1) to choose the forms of the $|\mathbf{u}|^2$ and $\nabla \mathbf{u}$ terms so as to satisfy the constraints (2.4.1) and (2.4.2), independent of the values of the coefficients $c^{(2)}$ and $c_\nabla^{(2)}$. In terms of (2.5.1), Eq. (2.4.1) yield immediately

$$f = n/6 \tag{2.5.3}$$

while (2.4.2) gives

$$c^{(1)} = 2 . \tag{2.5.4}$$

The specific values of $c^{(2)}$ and $c_\nabla^{(2)}$ can be determined only by explicit solution of the kinetic equation (2.3.5) including collision terms. (Some approximate results for these coefficients based on the Boltzmann transport equation will be given in Section 4.) Nevertheless, the structure of macroscopic equations can be derived from (2.5.1) without knowledge of the exact values of these parameters.

For a uniform equilibrium system with $\mathbf{u} = 0$, all the f_a are given by

$$f_a = f = n/6 . \tag{2.5.5}$$

In the case, the momentum flux tensor (2.4.9) is equal to the pressure tensor, given, as in the standard kinetic theory of gases, by

$$P_{ij} = \sum_a (\mathbf{e}_a)_i (\mathbf{e}_a)_j f = \frac{1}{2} n \delta_{ij} \tag{2.5.6}$$

where the second equality follows from Eq. (2.5.2). Note that this form is spatially isotropic, despite the underlying anisotropy of the cellular automaton lattice. This result can be deduced from general symmetry considerations, as discussed in Section 3. Equation (2.5.6) gives the equation of state relating the scalar pressure to the number density of the cellular automaton fluid:

$$p = n/2 . \tag{2.5.7}$$

When $\mathbf{u} \neq 0$, Π_{ij} can be evaluated in the approximation (2.5.1) using the relations

$$\sum_a (\mathbf{e}_a)_i (\mathbf{e}_a)_j (\mathbf{e}_a)_k = 0 \tag{2.5.8}$$

and

$$\sum_a (\mathbf{e}_a)_i (\mathbf{e}_a)_j (\mathbf{e}_a)_k (\mathbf{e}_a)_l = \frac{M}{d(d+2)} (\delta_{ij}\delta_{kl} + \delta_{ik}\delta_{jl} + \delta_{il}\delta_{jk}) . \tag{2.5.9}$$

The result is

$$\Pi_{ij} = \frac{n}{2}\delta_{ij} + \frac{n}{4} c^{(2)} \left[u_i u_j - \frac{1}{2} |\mathbf{u}|^2 \delta_{ij} \right] + \frac{n}{4} c_\nabla^{(2)} \left[\partial_i u_j - \frac{1}{2} \nabla \cdot \mathbf{u} \right] . \tag{2.5.10}$$

Substituting the result into Eq. (2.4.10), one obtains the final macroscopic equation

$$\begin{aligned}\partial_t(n\mathbf{u}) + \frac{1}{4}nc^{(2)}\left\{(\mathbf{u}\cdot\nabla)\mathbf{u} + \left[\mathbf{u}(\nabla\cdot\mathbf{u}) - \frac{1}{2}|\mathbf{u}|^2\right]\right\} \\ = -\frac{1}{2}\nabla n - \frac{1}{8}nc_\nabla^{(2)}\nabla^2\mathbf{u} - \frac{1}{4}\Xi\end{aligned} \tag{2.5.11}$$

where

$$\Xi = \mathbf{u}(\mathbf{u}\cdot\nabla)\left(nc^{(2)}\right) - \frac{1}{2}|\mathbf{u}|^2\nabla\left(nc^{(2)}\right) + (\mathbf{u}\cdot\nabla)\left(nc_\nabla^{(2)}\right) - \frac{1}{2}(\nabla\cdot\mathbf{u})\nabla\left(nc_\nabla^{(2)}\right). \tag{2.5.12}$$

The form (2.5.10) for Π_{ij} follows exactly from the Chapman-Enskog expansion (2.5.1). But to obtain Eq. (2.5.11), one must use the momentum equation (2.4.10). Equation (2.4.13) gives corrections to this equations that arise at second order in the lattice size parameter δ. These corrections must be compared with other effects included in Eq. (2.5.11). The rescaling $\mathbf{x} = \delta_x\mathbf{X}$ implies that spatial gradient terms in the Chapman-Enskog expansion can be of the same order as the $O(\delta_x)$ correction terms in Eq. (2.4.13). When the $\mathbf{e}_a\cdot\mathbf{u}$ term in the Chapman-Enskog expansion (2.5.1) for the f_a is substitute into the last term of Eq. (2.4.13), it gives a contribution[24]

$$\Psi = -\frac{1}{16}nc^{(1)}\nabla^2\mathbf{u} = -\frac{1}{8}n\nabla^2\mathbf{u} \tag{2.5.13}$$

to the right-hand side of Eq. (2.5.11). Note that Ψ depends solely on the choice of $\mathbf{e}_a$, and must, for example, vary purely linearly with the particle density f.

2.6. NAVIER-STOKES EQUATION

The standard Navier-Stokes equation for a continuum fluid in d dimensions can be written in the form

$$\partial_t(n\mathbf{u}) + \mu n(\mathbf{u}\cdot\nabla)\mathbf{u} = -\nabla p + \eta\nabla^2\mathbf{u} + \left(\zeta + \frac{1}{d}\eta\right)\nabla(\nabla\cdot\mathbf{u}) \tag{2.6.1}$$

where p is pressure, and η and ζ are, respectively, shear and bulk viscosities (e.g., Ref. 27). The coefficient μ of the convective term is usually constrained to have value 1 by Galilean invariance. Note that the coefficient of the last term in Eq. (2.6.1) is determined by the requirement that the term in Π_{ij} proportional to η be traceless.[27,57]

The macroscopic equation (2.5.11) for the cellular automaton fluid is close to the Navier-Stokes form (2.6.1). The convective and viscous terms are present, and have the usual structure. The pressure term appears according to the equation of state (2.5.7). There are, however, a few additional terms.

Terms proportional to $\mathbf{u}\nabla n$ must be discounted, since they depend on features of the microscopic distribution functions beyond those included in the Chapman-Enskog expansion (2.5.1). The continuity equation (2.4.7) shows that terms proportional to $\mathbf{u}(\nabla\cdot\mathbf{u})$ must also be neglected.

The term proportional to $\nabla|\mathbf{u}|^2$ remains, but can be combined with the ∇n term to yield an effective pressure term which includes fluid kinetic energy contributions.

The form of the viscous terms in (2.5.11) implies that for the cellular automaton fluid, considered here, the bulk viscosity is given by

$$\zeta = 0\,. \tag{2.6.2}$$

The value of η is determined by the coefficient $c_\nabla^{(2)}$ that appears in the microscopic distribution function (2.5.1), according to

$$\eta = n\nu = -\frac{1}{8}nc_\nabla^{(2)} \tag{2.6.3}$$

where ν is the kinematic viscosity. An approximate method of evaluating $c_\nabla^{(2)}$ is discussed in Section 4.6.

The convective term in Eq. (2.5.11) has the same structure as in the Navier-Stokes equation (2.6.1), but includes a coefficient

$$\mu = \frac{1}{4}c^{(2)} \tag{2.6.4}$$

which is not in general equal to 1. In continuum fluids, the covariant derivative usually has the form $D_t = \partial_t + \mathbf{u}\cdot\nabla$ implied by Galilean invariance. The cellular automaton fluid acts, however, as a mixture of components, each with velocities $\mathbf{e}_a$, and these components can contribute with different weights to the covariant derivatives of different quantities, leading to convective terms with different coefficients.

The usual coefficient of the convective term can be recovered in Eq. (2.6.1) and thus Eq. (2.5.11) by a simple rescaling in velocity: setting

$$\tilde{\mathbf{u}} = \mu\mathbf{u} \tag{2.6.5}$$

the equation for $\tilde{\mathbf{u}}$ has coefficient 1 for the $(\tilde{\mathbf{u}}\cdot\nabla)\tilde{\mathbf{u}}$ term.

Small perturbations from a uniform state may be represented by a linearized approximation to Eqs. (2.4.7) and (2.5.11), which has the standard sound wave equation form, with a sound speed obtained from the equation of state (2.5.7) as

$$c = 1/\sqrt{2}\,. \tag{2.6.6}$$

The form of the Navier-Stokes equation (2.6.1) is usually obtained by simple physical arguments. Detailed derivations suggest, however, that more elaborate equations may be necessary, particularly in two dimensions (e.g., Ref. 28). The Boltzmann approximation used in Section 4 yields definite values for $c^{(2)}$ and $c_\nabla^{(2)}$. Correlation function methods indicate, however, that additional effects yield logarithmically divergent contributions to $c_\nabla^{(2)}$ in two dimensions (e.g., Ref. 29). The full viscous term in this case may in fact be of the rough form $\nabla^2\log(\nabla^2)\mathbf{u}$.

2.7. HIGHER-ORDER CORRECTIONS

The derivation of the Navier-Stokes form (2.5.11) neglects all terms in the Chapman-Enskog expansion beyond those given explicitly in Eq. (2.5.1). This approximation is expected to be adequate only when $|\mathbf{u}| \ll c$. Higher-order corrections may be particularly significant for supersonic flows involving shocks (e.g., Ref. 30).

Since the dynamics of shocks are largely determined just by conservation laws (e.g., Ref. 27), they are expected to be closely analogous in cellular automaton fluids and in standard continuum fluids. For $|\mathbf{u}|/c \gtrsim 2$, however, shocks become so strong and thin that continuum descriptions of physical fluids can no longer be applied in detail (e.g., Ref. 14). The structure of shocks in such cases can apparently be found only through consideration of explicit particle dynamics.[11,14]

In the transonic flow regime $|\mathbf{u}| \approx c$, however, continuum equations may be used, but corrections to the Navier-Stokes form may be significant. A class of such corrections can potentially be found by maintaining terms $O(u^3)$ and higher in the Chapman-Enskog expansion (2.5.1).

In the homogeneous fluid approximation $\nabla \mathbf{u} = 0$, one may take

$$\begin{aligned} f_a = f\Big\{ & 1 + c^{(1)} \mathbf{e}_a \cdot \mathbf{u} + c^{(2)} \left[(\mathbf{e}_a \cdot \mathbf{u})^2 + \sigma_2 |\mathbf{u}|^2 \right] \\ & + c^{(3)} \left[(\mathbf{e}_a \cdot \mathbf{u})^3 + \sigma_3 |\mathbf{u}|^2 (\mathbf{e}_a \cdot \mathbf{u}) \right] \\ & + c^{(4)} \left[(\mathbf{e}_a \cdot \mathbf{u})^4 + \sigma_{4,1} |\mathbf{u}|^2 (\mathbf{e}_a \cdot \mathbf{u})^2 + \sigma_{4,2} |\mathbf{u}|^4 \right] + \cdots \Big\} \end{aligned} \tag{2.7.1}$$

The constraints (2.4.1) and (2.4.2) imply

$$c^{(1)} = d \tag{2.7.2}$$

$$\sigma_2 = -\frac{1}{d} \tag{2.7.3}$$

$$\sigma_3 = -\frac{3}{d+2} \tag{2.7.4}$$

$$\frac{3}{d(d+2)} + \frac{1}{d} \sigma_{4,1} + \sigma_{4,2} = 0 \tag{2.7.5}$$

where d is the space dimension, equal to two for the model of this section.

Corrections to (2.5.11) can be found by substituting (2.7.1) in the kinetic equation (2.4.8). For the hexagonal lattice model, one obtains, for example,

$$\begin{aligned} & \partial_t (n u_x) + \frac{1}{4} n c^{(2)} (u_x \partial_x u_x + u_x \partial_y u_y + u_y \partial_y u_x - u_y \partial_x u_y) \\ & + \frac{1}{8} n c^{(4)} \Big\{ \left[(5 + 4\sigma_{4,1}) u_x^3 - 3 u_x u_y^2 \right] \partial_x u_x \\ & + \left[(3 + 2\sigma_{4,1}) u_y^3 + (3 + 6\sigma_{4,1}) u_x^2 u_y \right] \partial_y u_x \\ & - \left[(3 + 4\sigma_{4,1}) u_y^3 + 3 u_x^2 u_y \right] \partial_x u_y \\ & + \left[(1 + 2\sigma_{4,1}) u_x^3 + (9 + 6\sigma_{4,1}) u_x u_y^2 \right] \partial_y u_y \Big\} = 0 . \end{aligned} \tag{2.7.6}$$

The $O(u^2)$ term in Eq. (2.7.6) has the isotropic form given in Eq. (2.5.11). The $O(u^4)$ term is, however, anisotropic.

To obtain an isotropic $O(u^4)$ term, one must generalize the model, as discussed in Section 3. One possibility is to allow vectors $\mathbf{e}_a$ corresponding to corners of an M-sided polygon with $M > 6$. In this case, the continuum equation deduced from the Chapman-Enskog expansion (2.7.1) becomes

$$\partial_t(n\mathbf{u}) + \frac{1}{4}nc^{(2)}\left[(\mathbf{u}\cdot\nabla)\mathbf{u} + \mathbf{u}(\nabla\cdot\mathbf{u}) - \frac{1}{2}\nabla|\mathbf{u}|^2\right] + \frac{1}{4}nc^{(4)}(1+\sigma_{4,1})\left\{|\mathbf{u}|^2\left[(\mathbf{u}\cdot\nabla)\mathbf{u} + \mathbf{u}(\nabla\cdot\mathbf{u}) - \nabla\mathbf{u}|^2\right] + \mathbf{u}(\mathbf{u}\cdot\nabla)|\mathbf{u}|^2\right\} = 0\,. \tag{2.7.7}$$

This gives a definite form for the next-order corrections to the convective part of the Navier-Stokes equation.

Corrections to the viscous part can be found by including terms proportional to $\nabla\mathbf{u}$ in the Chapman-Enskog expansion (2.7.1). The possible fourth-order terms are given by contractions of $u_i u_j \delta_k u_l$ with products of $(\mathbf{e}_a)_m$ or δ_{mn}. They yield a piece in the Chapman-Enskog expansion of the form

$$c_\nabla^{(4)}\left[\tau_1(\mathbf{e}_a\cdot\mathbf{u})^2(\mathbf{e}_a\cdot\nabla)(\mathbf{e}_a\cdot\mathbf{u}) + \tau_2|\mathbf{u}|^2(\mathbf{e}_a\cdot\nabla)(\mathbf{e}_a\cdot\mathbf{u}) + \tau_3(\mathbf{e}_a\cdot\mathbf{u})(\mathbf{u}\cdot\nabla)(\mathbf{e}_a\cdot\mathbf{u}) + \tau_4(\mathbf{e}_a\cdot\mathbf{u})^2(\nabla\cdot\mathbf{u}) + \tau_5|\mathbf{u}|^2(\nabla\cdot\mathbf{u})\right] \tag{2.7.8}$$

where Eq. (2.4.1) implies the constraints (for $d = 2$)

$$\tau_1 + 2\tau_3 = 0\,, \tag{2.7.9}$$

$$\tau_1 + 4\tau_2 + 4\tau_4 + 8\tau_5 = 0\,. \tag{2.7.10}$$

The resulting continuum equations may be written in terms of vectors formed by contractions of $u_i u_j \partial_k \partial_l u_m$ and $u_i \partial_j u_k \partial_l u_m$. The complete result is

$$
\begin{aligned}
&\partial_t(n\mathbf{u}) + \frac{1}{4}nc^{(2)}\left[(\mathbf{u}\cdot\nabla)\mathbf{u} + \mathbf{u}(\nabla\cdot\mathbf{u}) - \frac{1}{2}\nabla|\mathbf{u}|^2\right] \\
&\quad + \frac{1}{4}nc^{(4)}(1+\sigma_{4,1})\left\{|\mathbf{u}|^2\left[(\mathbf{u}\cdot\nabla)\mathbf{u} + \mathbf{u}(\nabla\cdot\mathbf{u}) - \nabla|\mathbf{u}|^2\right] + \mathbf{u}(\mathbf{u}\cdot\nabla)|\mathbf{u}|^2\right\} \\
&\quad = \frac{1}{8}nc_\nabla^{(2)}\nabla^2\mathbf{u} \\
&\qquad - \frac{1}{32}nc_\nabla^{(4)}\Bigg[\Big((\tau_1 - 4\tau_2 + 12\tau_4)\mathbf{u}(\nabla\cdot\mathbf{u})^2 - (\tau_1 - 4\tau_2 + 4\tau_4) \\
&\qquad \times \mathbf{u}\Big\{\nabla\left[(\mathbf{u}\cdot\nabla)\mathbf{u}\right] - (\mathbf{u}\cdot\nabla)(\nabla\cdot\mathbf{u})\Big\} + 8\tau_4\Big\{\left[(\mathbf{u}\cdot\nabla)\mathbf{u}\right]\cdot\nabla\Big\}\mathbf{u} \\
&\qquad + \frac{1}{2}(\tau_1 + 4\tau_2)\left[(\nabla|\mathbf{u}|^2)\cdot\nabla\right]\mathbf{u} \\
&\qquad + 2\tau_1\mathbf{u}\left[\frac{1}{2}\nabla\cdot(\nabla|\mathbf{u}|^2) - \mathbf{u}\cdot(\nabla^2\mathbf{u})\right] - 4\tau_4(\nabla\cdot\mathbf{u})\nabla|\mathbf{u}|^2\Big) \\
&\qquad + \Bigg\{8\tau_4\left[\mathbf{u}(\mathbf{u}\cdot\nabla)(\nabla\cdot\mathbf{u}) - \frac{1}{2}|\mathbf{u}|^2\nabla(\nabla\cdot\mathbf{u})\right] \\
&\qquad + 2\tau_1\mathbf{u}\left[\mathbf{u}\cdot(\nabla^2\mathbf{u})\right] + 4\tau_2|\mathbf{u}|^2\nabla^2\mathbf{u}\Bigg\}\Bigg]
\end{aligned}
\tag{2.7.11}
$$

where, on the right-hand side, the first group of terms are all $O((\nabla\mathbf{u})^2)$, while the second group are $O(\nabla\nabla\mathbf{u})$. Further corrections involve higher derivative terms, such as $u_i\partial_j\partial_k\partial_l u_m$. For a channel flow with $u_x = ax^2$, $u_y = 0$, the time time-independent terms in Eq. (2.7.11) have an x component

$$
\frac{1}{4}ac_\nabla^{(2)} + \frac{5}{8}a^3x^4c_\nabla^{(4)}(\tau_1 + 2\tau_2 + 2\tau_4) + \frac{1}{2}a_2x^3c^{(2)} + a^4x^7x^{(4)}(1+\sigma_{4,1}) \tag{2.7.12}
$$

and zero y component.

3. SYMMETRY CONSIDERATIONS

3.1. TENSOR STRUCTURE

The form of the macroscopic equations (2.4.7) and (2.5.11) depends on few specific properties of the hexagonal lattice cellular automaton model. The most important properties relate to the symmetries of the tensors

$$\mathbf{E}^{(n)}_{i_1 i_2 \cdots i_n} = \sum_a (\mathbf{e}_a)_{i_1} \cdots (\mathbf{e}_a)_{i_n} . \tag{3.1.1}$$

These tensors are determined in any cellular automaton fluid model simply from the choice of the basic particle directions $\mathbf{e}_a$. The momentum flux tensor (2.4.9) is given in terms of them by

$$\begin{aligned} \Pi_{ij} = & f\Bigg(\mathbf{E}^{(2)}_{ij} + c^{(1)} \mathbf{E}^{(3)}_{ijk} u_k + c^{(2)} \left[\mathbf{E}^{(4)}_{ijkl} u_k u_l + \sigma \mathbf{E}^{(2)}_{ij} u_k u_k \right] \\ & c^{(2)}_{\nabla} \left[\mathbf{E}^{(4)}_{ijkl} \partial_k u_l + \sigma \mathbf{E}^{(2)}_{ij} \partial_k u_k \right] \Bigg) \end{aligned} \tag{3.1.2}$$

where repeated indices are summed, and to satisfy the conditions (2.4.1) and (2.4.2)

$$\sigma = -\mathbf{E}^{(4)}_{ijkk} / \mathbf{E}^{(2)}_{ij} . \tag{3.1.3}$$

The basic condition for standard hydrodynamic behavior is that the tensors $\mathbf{E}^{(n)}$ for $n \leq 4$ which appear in (3.1.2) should be isotropic. From the definition (3.1.1), the tensors must always be invariant under the discrete symmetry group of the underlying cellular automaton array. What is needed is that they should in addition be invariant under the full continuous rotation group.

The definition (3.1.1) implies that the $\mathbf{E}^{(n)}$ must be totally symmetric in their space indices. With no further conditions, the $\mathbf{E}^{(n)}$ could have $\binom{n+d-1}{n}$ independent components in d space dimensions. Symmetries in the underlying cellular automaton array provide constraints which can reduce the number of independent components.

Tensors that are invariant under all rotations and reflections (or inversions) can have only one independent component. Such invariance is obtained with a continuous set of vectors $\mathbf{e}_a$ uniformly distributed on the unit sphere. Invariance up to finite n can also be obtained with certain finite sets of vectors $\mathbf{e}_a$.

Isotropic tensors $\mathbf{E}^{(n)}$ obtained with sets of M vectors $\mathbf{e}_a$ in d space dimensions must take the form

$$\mathbf{E}^{(2n+1)} = 0 \tag{3.1.4}$$

$$\mathbf{E}^{(2n)} = \frac{M}{d(d+2)\cdots(d+2n-2)} \Delta^{(2n)} \tag{3.1.5}$$

where

$$\Delta^{(2)}_{ij} = \delta_{ij} \tag{3.1.6}$$

$$\Delta^{(4)}_{ijkl} = \delta_{ij}\delta_{kl} + \delta_{ik}\delta_{jl} + \delta_{il}\delta_{jk} \tag{3.1.7}$$

and in general $\Delta^{(2n)}$ consists of a sum of all the $(2n-1)!!$ possible products of Kronecker delta symbols of pairs on indices, given by the recursion relation

$$\Delta^{(2n)}_{i_1 i_2 \cdots i_{2n}} = \sum_{j=2}^{2n} \delta_{i_1 i_j} \Delta^{(2n-2)}_{i_2 \cdots i_{j-1} i_{j+1} \cdots i_{2n}} . \tag{3.1.8}$$

The form of the $\Delta^{(2n)}$ can also be specified by giving their upper simplicial components (whose indices form a nonincreasing sequence). Thus, in two dimensions,

$$\Delta^{(4)} = [3,0,1,0,3] \tag{3.1.9}$$

where the 1111, 2111, 2211, 2221, and 2222 components are given. In three dimensions,

$$\Delta^{(4)} = [3,0,1,0,3,0,0,0,0,1,0,1,0,0,3] . \tag{3.1.10}$$

Similarly,

$$\Delta^{(6)} = [5,0,1,0,1,0,5] \tag{3.1.11}$$

and

$$\Delta^{(6)} = [15,0,3,0,3,0,15,0,0,0,0,0,0,3,0,1,0,3,0,0,0,0,3,0,3,0,0,15] \tag{3.1.12}$$

in two and three dimensions, respectively.

For isotropic sets of vectors $\mathbf{e}_a$, one finds from (3.1.5)

$$\frac{1}{M}\sum_a (\mathbf{e}_a \cdot \mathbf{v})^{(2n)} = Q_{2n}|\mathbf{v}|^{2n} = \frac{(2n-1)!!}{d(d+2)\cdots(d+2n-2)}|\mathbf{v}|^{2n} \tag{3.1.13}$$

so that for $d = 2$

$$Q_2 = \frac{1}{2}, \qquad Q_4 = \frac{3}{8}, \qquad Q_6 = \frac{5}{16}, \qquad Q_8 = \frac{35}{128} \tag{3.1.14}$$

while for $d = 3$

$$Q_{2n} = \frac{1}{2n+1} . \tag{3.1.15}$$

Similarly,

$$\frac{1}{M}\sum_a (\mathbf{e}_a \cdot \mathbf{v})^{2n} \mathbf{e}_a \cdot \mathbf{v} = Q_{2n}|\mathbf{v}|^{2n}\mathbf{v} . \tag{3.1.16}$$

In the model of Section 2, all the particle velocities $\mathbf{e}_a$ are fundamentally equivalent, and so are added with equal weight in the tensor (3.1.1). In some cellular automaton fluid models, however, one may, for example, allow particle velocities $\mathbf{e}_a$ with unequal magnitudes (e.g., Ref. 31). The relevant tensors in such cases are

$$\mathbf{E}^{(n)}_{i_1 i_2 \cdots i_n} = \sum_a w(|\mathbf{e}_a|^2)(\mathbf{e}_a)_{i_1} \cdots (\mathbf{e}_a)_{i_n} \tag{3.1.17}$$

where the weights $w(|\mathbf{e}_a|^2)$ are typically determined from coefficients in the Chapman-Enskog expansion.

3.2. POLYGONS

As a first example, consider a set of unit vectors $\mathbf{e}_a$ corresponding to the vertices of a regular M-sided polygon:

$$\mathbf{e}_a = \left(\cos\frac{2\pi a}{M}, \sin\frac{2\pi a}{M}\right) \tag{3.2.1}$$

For sufficiently large M, any tensor $\mathbf{E}^{(n)}$ constructed from these $\mathbf{e}_a$ must be isotropic. Table 1 gives the conditions on M necessary to obtain isotropic $\mathbf{E}^{(n)}$. In general, it can be shown that $\mathbf{E}^{(n)}$ is isotropic if and only if M does not divide any integers $n, n-2, n-4, \ldots$.[32] Thus, for example, $\mathbf{E}^{(n)}$ must be isotropic whenever $n > M$.

In the case $M = 6$, corresponding to the hexagonal lattice considered in Section 2, the $\mathbf{E}^{(n)}$ are isotropic up to $n = 5$. The macroscopic equations obtained in this case thus have the usual hydrodynamic form. However, a square lattice, with $M = 4$, yields an anisotropic $\mathbf{E}^{(4)}$, given by

$$\mathbf{E}^{(4)}|_{M=4} \; 2\delta^{(4)} \tag{3.2.2}$$

where $\delta^{(n)}$ is the Kronecker delta symbol with n indices. The macroscopic equation obtained in this case is

$$\begin{aligned}\delta_t(nu_x) + \frac{1}{2}nc^{(2)}(u_x\partial_x u_x - u_y\partial_x u_y) \\ = -\frac{1}{2}\partial_x n - \frac{1}{8}nc_\nabla^{(2)}(\partial_{xx}u_x - \partial_{xy}u_y) - \frac{1}{4}(u_x^2 - u_y^2)\partial_x\left(nc^{(2)}\right) \\ - \frac{1}{8}(\partial_x u_x - \partial_y u_y)\partial_x\left(nc_\nabla^{(2)}\right)\end{aligned}$$

TABLE 1 Conditions for the Tensors $\mathbf{E}^{(n)}$ of Eq. (3.1.1) to be Isotropic with the Lattice Vectors $\mathbf{e}_a$ chosen to Correspond to the Vertices of Regular M-Sided Polygons

$\mathbf{E}^{(2)}$	$M > 2$
$\mathbf{E}^{(3)}$	$M \geq 2, M \neq 3$
$\mathbf{E}^{(4)}$	$M > 2, M \neq 4$
$\mathbf{E}^{(5)}$	$M \geq 2, M \neq 3, 5$
$\mathbf{E}^{(6)}$	$M > 4, M \neq 6$
$\mathbf{E}^{(7)}$	$M \geq 2, M \neq 3, 5, 7$

TABLE 2 Isotropy of the Tensors $\mathbf{E}^{(n)}$ with $\mathbf{e}_a$ Chosen as the M Vertices of Regular Polyhedra[1]

	$\mathbf{e}_a$	M	$\mathbf{E}^{(2)}$	$\mathbf{E}^{(3)}$	$\mathbf{E}^{(4)}$	$\mathbf{E}^{(5)}$	$\mathbf{E}^{(6)}$
Tetrahedron	$(1,1,1)$, cyc: $(1,-1,-1)$	4	Y	N	N	N	N
Cube	$(\pm1,\pm1,\pm1)$	8	Y	Y	N	Y	N
Octahedron	cyc: $(\pm1,0,0)$	6	Y	Y	N	Y	N
Dodecahedron	$(\pm1,\pm1,\pm1)$, cyc: $(0,\pm\phi^{-1},\pm\phi)$	20	Y	Y	Y	Y	N
Icosahedron	cyc: $(0,\pm\phi,\pm1)$	12	Y	Y	Y	Y	N

[1] In the forms for $\mathbf{e}_a$ (which are given without normalization), the notation "cyc:" indicates all cyclic permutations. (All possible combinations of signs are chosen in all cases.) ϕ is the golden ratio $(1+\sqrt{5})/2 \approx 1.618$.

which does not have the standard Navier-Stokes forms.[6][3]

On a hexagonal lattice, $\mathbf{E}^{(4)}$ is isotropic, but $\mathbf{E}^{(6)}$ has the component form

$$\mathbf{E}^{(6)}\,|_{M=6} = \frac{1}{16}[33,0,3,0,9,0,27] \tag{3.2.4}$$

which differs from the isotropic result (3.1.11). The corrections (2.7.6) to the Navier-Stokes equation are therefore anisotropic in this case.

3.3. POLYHEDRA

As three-dimensional examples, one can consider vectors $\mathbf{e}_a$ corresponding to the vertices of regular polyhedra. Only for the five Platonic solids are all the $|\mathbf{e}_a|^2$ equal. Table 2 gives results for the isotropy of the $\mathbf{E}^{(n)}$ in these cases. Only for the icosahedron and dodecahedron is $\mathbf{E}^{(4)}$ found to be isotropic, so that the usual hydrodynamic equations are obtained. As in two dimensions, the $\mathbf{E}^{(2n)}$ for the cube are all proportional to a single Kronecker delta symbol over all indices.

In five and higher dimensions, the only regular polytopes are the simplex, and the hypercube and its dual.[34] These give isotropic $\mathbf{E}^{(n)}$ only for $n < 3$, and for $n < 4$ and $n < 4$, respectively.

In four dimensions, there are three additional regular polytopes,[34] specified by Schlafi symbols $\{3,4,3\}$, $\{3,3,5\}$, and $\{5,3,3\}$. (The elements of these lists

[3]Note that even the linearized equation for sound waves is anisotropic on a square lattice. The waves propagate isotropically, but are damped with an effective viscosity that varies with direction, and can be negative.[33]